Overall elastic properties of composites from optimal strong contrast expansion

Quy-Dong To, Minh Tan Nguyen, Guy Bonnet, Vincent Monchiet, Viet Thanh To

Overall elastic properties of composites from optimal strong contrast expansion

Quy-Dong To[a,b,c,*], Minh-Tan Nguyen[c,d], Guy Bonnet[c], Vincent Monchiet[c], Viet-Thanh To[d]

[a] Division of Construction Computation, Institute for Computational Science, Ton Duc Thang University, Ho Chi Minh City, Vietnam
[b] Faculty of Civil Engineering, Ton Duc Thang University, Ho Chi Minh City, Vietnam
[c] Université Paris-Est, Laboratoire Modélisation et Simulation Multi Echelle, MSME UMR 8208 CNRS, 5 Boulevard Descartes, 77454 Marne-la-Vallée Cedex 2, France
[d] Le Quy Don Technical University, 236 Hoang Quoc Viet, Bac Tu Liem, Ha Noi, Vietnam

ABSTRACT

In this paper, we propose a new systematic procedure of estimating elastic properties of composites constituted of two phases, matrix and inclusions. A class of integral equations based on eigenstrain (or eigenstress) with the matrix as reference material is constructed with an explicit form in Fourier space. Each integral equation belonging to this class can yield estimates of the overall elastic tensor via Neumann series expansion. The best estimates and series are selected based on the convergence rate criteria of the series, i.e the spectral radius must be minimized. The optimized series is convergent for any finite contrast between inclusions and matrix. Applying the optimized series and the associated estimates to different microstructures yields very satisfying results when compared with the related full solution. For the case of a random distribution of spherical inclusions, exact relations between the elastic tensor and nth order structure factors are demonstrated.

Keywords:
Triplet structure factor
Optimized Neumann series
Integral equation
Fourier transform
Spectral radius

1. Introduction

We consider the problem of finding the effective stiffness tensor $\mathbb{C}^e$ of periodic heterogeneous matrix-inclusion materials. The existence of $\mathbb{C}^e$ and homogenization procedure have been rigorously founded in the literature (Sanchez-Palencia, 1980). Given the distribution of the constituents, the cell problem must be solved first and the linear relation between average stress and strain is then established. Estimates can be obtained by making relevant approximation to the ingredients constituting the effective tensor (see e.g Eshelby, 1957; Christensen and Lo, 1979; Mori and Tanaka, 1973). Although the present contribution concerns the theory of optimally estimating $\mathbb{C}^e$ from the microstructure, it is closely related to FFT numerical homogenization methods.

By introducing a reference material $\mathbb{C}^0$, the heterogeneity effect can be viewed as a distribution of eigenstrains within an homogeneous material. Using the related Green tensor, our problem can be formulated as a Lippmann-Schwinger equation for eigenstrain (Nemat-Nasser et al., 1982). The integral equation is at the origin of resolution methods based on iteration and Fast Fourier Transform (FFT) techniques (Michel et al., 1999; Bhattacharya and Suquet, 2005). Significant progresses have been made regarding the improvement of convergence rate (Michel et al., 1999; Eyre and Milton, 1999; Milton, 2002; Monchiet and Bonnet, 2012; Brisard and Dormieux, 2010). The study of convergence rate in those works will be extended in the present contribution in the case of new integral equations.

We can remark that the iteration scheme used to solve the Lippmann–Schwinger equation corresponds to the Neumann series summation. The latter can be used to derive exact theoretical relations and estimates (see e.g Torquato, 2001; Milton, 2002, and the references therein), using for example the weak and strong contrast expansions. As an extension to previous works on conductivity, Torquato (1998); 1997) introduced the cavity strain field and derived the strong contrast estimates. Connections with statistical information related to the distribution of two phases, the n point correlation function, were also demonstrated in this context. At the second order, the estimates produce satisfying results for systems composed of dispersed non overlapping spheres. However, the series of Torquato is increasingly complicated at higher order without guarantee of convergence. As already shown in Milton (2002), the starting point of the strong contrast expansion is a conditionally convergent series. In a similar way, bounds of the effective elasticity tensor are also depending on correlation functions (see

* Corresponding author.
E-mail addresses: toquydong@tdt.edu.vn, quy-dong.to@u-pem.fr (Q.-D. To).

Milton, 2002, pps 313, 554) and in this context, the use of the matrix as a reference material simplifies significantly the expression of these bounds

In this paper, we propose a new estimate based on a series expansion that works at all finite contrast ratio, while using the matrix as a reference material. Additionally, we can control and optimize the convergence rate so that the series converges in the quickest way, and therefore produces the best estimate when using a finite sum in the series expansion. A class of integral equations for eigenstrain depending on two parameters α, β is first derived. The spectral radius and norm of the corresponding operators are bounded by analytical expressions. Different optimization methods are proposed to find the fastest series convergence and the associated estimates. It is noteworthy that *a convergence will be obtained for any finite contrast between matrix and inclusions, while using always the matrix as a reference material, which simplifies significantly the series expansion*.

Similarly to the estimations of the effective elasticity tensor using correlation functions (Milton, 2002; Torquato, 2001), the new method presented in this paper allows to *estimate the effective elasticity tensor using the n order structure factors*, which represent the counterpart in Fourier space of correlation functions. As an example, a direct connection of the effective elasticity tensor to nth order structure factors is given in the case of randomly distributed spheres. Numerical applications for cubic arrays and random distribution of spheres yield very good results in comparison with FFT based methods and other results from the literature. The details of those contributions are presented in the following.

2. Mathematical preliminaries

As it will be seen in the following sections, the problem of the convergence of the Neumann series associated to a given integral equation is related to the spectrum of a fourth order iteration tensor which appears in the integral equation. In this section, the notations and mathematical results related to these fourth order tensors will be presented.

2.1. Notations and definitions

Before proceeding to the considerations on the spectrum of fourth order operators, we introduce first the system of abstracted notations and some important definitions which will be used throughout the paper. Most of our calculations involve symmetric second order tensors and fourth order tensors with minor symmetries. Unless specified, two tensors standing next to each other implies their double contraction product. Given two fourth order tensors $\mathbb{A}$ and $\mathbb{B}$ and two second order tensors $\boldsymbol{u}$ and $\boldsymbol{v}$, the double contraction products $\mathbb{A}\mathbb{B}$, $\mathbb{A}\boldsymbol{u}$ and $\boldsymbol{u}\boldsymbol{v}$ read

$$\begin{aligned}&(\mathbb{A}\mathbb{B})_{ijkl} = A_{ijmn}B_{nmkl}, \quad (\mathbb{A}\boldsymbol{u})_{ij} = A_{ijkl}u_{lk},\\ &\boldsymbol{u}\boldsymbol{v} = u_{ij}v_{ji}, \quad i,j,k,l = 1,2,3\end{aligned} \tag{1}$$

The symbol $\otimes$ denotes the usual tensorial product and $\underline{\overline{\otimes}}$ a special symmetrized tensorial product between two second order tensors $\boldsymbol{u}$ and $\boldsymbol{v}$

$$\begin{aligned}&(\boldsymbol{u}\underline{\overline{\otimes}}\boldsymbol{v})_{ijkl} = \frac{1}{2}(u_{ik}v_{jl} + u_{il}v_{jk}), \quad (\boldsymbol{u}\otimes\boldsymbol{v})_{ijkl} = u_{ij}v_{kl},\\ &i,j,k,l = 1,2,3.\end{aligned} \tag{2}$$

We are also dealing with periodic functions using Fourier analysis. Any $V-$periodic tensor field $\boldsymbol{u}$, function of coordinate $\boldsymbol{x}(x_1, x_2, x_3)$ can be expressed as an infinite Fourier series

$$\boldsymbol{u}(\boldsymbol{x}) = \sum_{\boldsymbol{\xi}} \boldsymbol{u}(\boldsymbol{\xi})e^{i\boldsymbol{\xi}\boldsymbol{x}}, \tag{3}$$

with $\boldsymbol{u}(\boldsymbol{\xi})$ being the Fourier transform of $\boldsymbol{u}(\boldsymbol{x})$

$$\boldsymbol{u}(\boldsymbol{\xi}) = \frac{1}{V}\int_V \boldsymbol{u}(\boldsymbol{x})e^{-i\boldsymbol{\xi}\boldsymbol{x}}d\boldsymbol{x}, \quad \forall\boldsymbol{\xi}. \tag{4}$$

In (3), the sum is taken over all the wavevectors $\boldsymbol{\xi}$ whose components ξ_1, ξ_2 and ξ_3 are defined from the relation

$$\xi_i = \frac{2\pi n_i}{l_i}, \quad i = 1,2,3, \quad n_1, n_2, n_3 \in \mathbb{Z}, \tag{5}$$

where l_1, l_2, l_3 are the periods along the three directions, i.e the dimensions of the unit cell V. According to the convolution theorem, products in Fourier space correspond to convolution products, (notation *, in physical space) by

$$[\mathbb{A} * \boldsymbol{u}](\boldsymbol{\xi}) = \mathbb{A}(\boldsymbol{\xi})\boldsymbol{u}(\boldsymbol{\xi}), \tag{6}$$

In the paper, we will encounter frequently equations in the form

$$\boldsymbol{u} = \boldsymbol{U} + \mathbb{A} * \boldsymbol{u} \tag{7}$$

for a given second order tensorial function $\boldsymbol{U}(\boldsymbol{x})$ and fourth order tensorial operator $\mathbb{A}$. The solution $\boldsymbol{u}$ of the above equation is the following Neumann series

$$\boldsymbol{u} = \sum_{n=0}^{\infty}(\mathbb{A}*)^n\boldsymbol{U}. \tag{8}$$

Numerically, the above summation is equivalent to repeating the iterative scheme

$$\boldsymbol{u}^0 = \boldsymbol{U}, \quad \boldsymbol{u}^{n+1} = \boldsymbol{U} + \mathbb{A} * \boldsymbol{u}^n. \tag{9}$$

until convergence. The convergence rate of the Neumann series (or the iterative scheme) can be estimated from the spectral radius or the norm of the associated operator $\mathbb{A}$. The spectral radius of an operator $\mathbb{A}$ is the absolute maximum of all eigenvalues λ

$$\rho(\mathbb{A}) = \max|\lambda| : \quad \exists\boldsymbol{u}, \quad \mathbb{A} * \boldsymbol{u} = \lambda\boldsymbol{u}, \quad \text{or} \quad \mathbb{A}(\boldsymbol{\xi})\boldsymbol{u}(\boldsymbol{\xi}) = \lambda\boldsymbol{u}(\boldsymbol{\xi}) \tag{10}$$

The set of symmetric second order tensors has the structure of an Hilbert space related to the scalar product between two second order tensor fields, notation $\langle .,. \rangle$

$$\langle \boldsymbol{u}, \boldsymbol{v}\rangle = \frac{1}{V}\int_V \boldsymbol{u}(\boldsymbol{x})\boldsymbol{v}(\boldsymbol{x})d\boldsymbol{x} = \sum_{\boldsymbol{\xi}} \boldsymbol{u}(\boldsymbol{\xi})\overline{\boldsymbol{v}(\boldsymbol{\xi})}, \tag{11}$$

where the overline notation $\overline{.}$ stands for the complex conjugate value. Consequently, the related norm, notation $\|.\|$, of any tensor field $\boldsymbol{u}(\boldsymbol{x})$ can be defined by the expression

$$\|\boldsymbol{u}\| = \sqrt{\langle \boldsymbol{u}, \boldsymbol{u}\rangle}. \tag{12}$$

The norm of operator $\mathbb{A}$ is then defined as

$$\|\mathbb{A}\| = \inf\{c \geq 0 : \|\mathbb{A} * \boldsymbol{u}\| \leq c\|\boldsymbol{u}\|\} \tag{13}$$

and in the Hilbert space, it can be evaluated as

$$\|\mathbb{A}\| = \sqrt{\rho(\mathbb{A}^\dagger\mathbb{A})}, \quad A_{ijkl}(\boldsymbol{\xi}) = \overline{A^\dagger_{klij}(\boldsymbol{\xi})} \tag{14}$$

with $\mathbb{A}^\dagger$ being the adjoint operator of $\mathbb{A}$. The norm and the spectral radius meet the inequality

$$\rho(\mathbb{A}) \leq \|\mathbb{A}\|, \tag{15}$$

where the equality is achieved if $\mathbb{A}$ is self-adjoint or at least normal, i.e $\mathbb{A}^\dagger\mathbb{A} = \mathbb{A}\mathbb{A}^\dagger$.

2.2. Walpole base

We consider operators which are transversely isotropic fourth order tensors in Fourier space and have minor symmetries, the plane of isotropy being normal to the wave vector $\boldsymbol{\xi}$. The related unit direction vector along $\boldsymbol{\xi}$ is denoted as $\overline{\boldsymbol{\xi}}$. It has been shown by Walpole (1981) that these tensors are a linear combination of the following six tensors which constitute the Walpole base:

$$\begin{aligned}&\mathbb{E}_1 = \frac{1}{2}\boldsymbol{k}^\perp \otimes \boldsymbol{k}^\perp, \quad \mathbb{E}_2 = \boldsymbol{k} \otimes \boldsymbol{k}, \quad \mathbb{E}_3 = \boldsymbol{k}^\perp \underline{\otimes} \boldsymbol{k}^\perp - \mathbb{E}_1,\\ &\mathbb{E}_4 = \boldsymbol{k}^\perp \underline{\otimes} \boldsymbol{k} + \boldsymbol{k} \underline{\otimes} \boldsymbol{k}^\perp, \quad \mathbb{E}_5 = \boldsymbol{k} \otimes \boldsymbol{k}^\perp, \quad \mathbb{E}_6 = \boldsymbol{k}^\perp \otimes \boldsymbol{k},\end{aligned} \tag{16}$$

where $\boldsymbol{k}$ and $\boldsymbol{k}^\perp$ are the second order projection tensors

$$\boldsymbol{k} = \overline{\boldsymbol{\xi}} \otimes \overline{\boldsymbol{\xi}}, \quad \boldsymbol{k}^\perp = \boldsymbol{I} - \boldsymbol{k}, \tag{17}$$

and $\boldsymbol{I}$ the second order identity tensor. As shown later, most of our calculations involve transversely isotropic tensors (Green tensors in Fourier space) and constant isotropic tensors (elasticity tensors of isotropic constituents). Those calculations can be considerably simplified using Walpole base elements. For example, the fourth order identity tensor $\mathbb{I}$ and the spherical and deviatoric projection tensors $\mathbb{J}$ and $\mathbb{K}$ can be expressed in the Walpole base in the form

$$\begin{aligned}&\mathbb{I} = \mathbb{E}_1 + \mathbb{E}_2 + \mathbb{E}_3 + \mathbb{E}_4,\\ &\mathbb{J} = \frac{1}{3}\boldsymbol{I} \otimes \boldsymbol{I} = \frac{1}{3}(2\mathbb{E}_1 + \mathbb{E}_2 + \mathbb{E}_5 + \mathbb{E}_6),\\ &\mathbb{K} = \mathbb{I} - \mathbb{J} = \frac{1}{3}(\mathbb{E}_1 + 2\mathbb{E}_2 - \mathbb{E}_5 - \mathbb{E}_6) + \mathbb{E}_3 + \mathbb{E}_4.\end{aligned} \tag{18}$$

Given any two transversely isotropic tensors $\mathbb{A}$ and $\mathbb{B}$ in the Walpole base

$$\begin{aligned}&\mathbb{A} = a_1\mathbb{E}_1 + a_2\mathbb{E}_2 + a_3\mathbb{E}_3 + a_4\mathbb{E}_4 + a_5\mathbb{E}_5 + a_6\mathbb{E}_6,\\ &\mathbb{B} = b_1\mathbb{E}_1 + b_2\mathbb{E}_2 + b_3\mathbb{E}_3 + b_4\mathbb{E}_4 + b_5\mathbb{E}_5 + b_6\mathbb{E}_6,\end{aligned} \tag{19}$$

their double inner product can be computed via the formula

$$\begin{aligned}\mathbb{A}\mathbb{B} = {}&(a_1b_1 + 2a_6b_5)\mathbb{E}_1 + (a_2b_2 + 2a_5b_6)\mathbb{E}_2 + a_3b_3\mathbb{E}_3 + a_4b_4\mathbb{E}_4\\ &+(a_2b_5 + a_5b_1)\mathbb{E}_5 + (a_1b_6 + a_6b_2)\mathbb{E}_6.\end{aligned} \tag{20}$$

These properties are important for the calculation of the spectral radius or norm, which will be presented in the later sections. From the definition of the adjoint operator in the previous section, we can also deduce that

$$\mathbb{E}_i^\dagger = \mathbb{E}_i, \quad \forall i = 1, 2, 3, 4, \quad \mathbb{E}_6^\dagger = \mathbb{E}_5, \quad \mathbb{E}_5^\dagger = \mathbb{E}_6. \tag{21}$$

In other words, the operators $\mathbb{E}_1, \mathbb{E}_2, \mathbb{E}_3$ and $\mathbb{E}_4$ are self-adjoint and the operators $\mathbb{E}_5$ and $\mathbb{E}_6$ are adjoint operators of each other. The fourth order operator $\mathbb{A}$ is self-adjoint if its components along $\mathbb{E}_5$ and $\mathbb{E}_6$ are identical.

2.3. Spectral radius and norm of operators via Walpole base

Always working in Fourier space, we shall determine the eigenvalues of $\mathbb{A}(\boldsymbol{\xi})$ in the form (19). Multiplying both sides of the eigen Eq. (10) with $\mathbb{E}_i$ $i = 1, 2, .., 6$, and then with $\boldsymbol{v}$, we have a system of linear equations

$$\begin{cases} a_1(\boldsymbol{v}\mathbb{E}_1\boldsymbol{v}) + a_6(\boldsymbol{v}\mathbb{E}_6\boldsymbol{v}) = \lambda(\boldsymbol{v}\mathbb{E}_1\boldsymbol{v})\\ a_2(\boldsymbol{v}\mathbb{E}_2\boldsymbol{v}) + a_5(\boldsymbol{v}\mathbb{E}_5\boldsymbol{v}) = \lambda(\boldsymbol{v}\mathbb{E}_2\boldsymbol{v})\\ a_3(\boldsymbol{v}\mathbb{E}_3\boldsymbol{v}) = \lambda(\boldsymbol{v}\mathbb{E}_3\boldsymbol{v})\\ a_4(\boldsymbol{v}\mathbb{E}_4\boldsymbol{v}) = \lambda(\boldsymbol{v}\mathbb{E}_4\boldsymbol{v})\\ a_1(\boldsymbol{v}\mathbb{E}_5\boldsymbol{v}) + 2a_6(\boldsymbol{v}\mathbb{E}_2\boldsymbol{v}) = \lambda(\boldsymbol{v}\mathbb{E}_5\boldsymbol{v})\\ a_2(\boldsymbol{v}\mathbb{E}_6\boldsymbol{v}) + 2a_5(\boldsymbol{v}\mathbb{E}_1\boldsymbol{v}) = \lambda(\boldsymbol{v}\mathbb{E}_6\boldsymbol{v}) \end{cases} \tag{22}$$

It turns out that the vector of components $\boldsymbol{v}\mathbb{E}_i\boldsymbol{v}$ with $i = 1, 2, ..6$ is an eigenvector of the matrix built with the elements a_i appearing in the left side of (22) and λ is an eigenvalue of this matrix. As a result, λ must be the solution of the eigen equation

$$\begin{vmatrix} a_1-\lambda & 0 & 0 & 0 & 0 & a_6\\ 0 & a_2-\lambda & 0 & 0 & a_5 & 0\\ 0 & 0 & a_3-\lambda & 0 & 0 & 0\\ 0 & 0 & 0 & a_4-\lambda & 0 & 0\\ 0 & 2a_6 & 0 & 0 & a_1-\lambda & 0\\ 2a_5 & 0 & 0 & 0 & 0 & a_2-\lambda \end{vmatrix} = 0 \tag{23}$$

or

$$(a_3 - \lambda)(a_4 - \lambda)[(a_1 - \lambda)(a_2 - \lambda) - 2a_5a_6]^2 = 0. \tag{24}$$

Finding the roots of Eq. (24) yields the values for λ and the spectral radius of $\mathbb{A}$ can now be computed with the formula

$$\rho(\mathbb{A}) = \max\left\{|a_3|, |a_4|, \frac{1}{2}|(a_1 + a_2) \pm \sqrt{(a_1 - a_2)^2 + 8a_5a_6}|\right\}. \tag{25}$$

Applying the same procedure as before to find the eigenvalues of $\mathbb{A}^\dagger\mathbb{A}$, we can determine $\|\mathbb{A}\|$

$$\begin{aligned}\|\mathbb{A}\| = \sqrt{\rho(\mathbb{A}^\dagger\mathbb{A})} = \max\{&|a_3|, |a_4|,\\ &\frac{1}{2}\left[\sqrt{(a_1-a_2)^2+2(a_5+a_6)^2}+\sqrt{(a_1+a_2)^2+2(a_5-a_6)^2}\right]\Big\}.\end{aligned} \tag{26}$$

3. Homogenization of elastic periodic composites

The computation of effective properties of composites can be expressed in the real space. However, one important ingredient of the homogenization process is the use of Green's tensors which are highly singular in the real space, while their Fourier transforms can be expressed analytically in a simple way. In addition, it will be shown that the use of the formulation in Fourier space introduces naturally the structure factors which are related to the geometrical distribution of the component materials. As a result, the formulation will be done jointly in real space and in Fourier space. In a first step, the homogenization problem will be expressed by using integral equations. Next, the optimization of the solution of these integral equations by using Neumann series will be studied.

3.1. Governing integral equations

We consider a heterogeneous material where the local isotropic stiffness $\mathbb{C}(\boldsymbol{x})$ (compliance $\mathbb{S}(\boldsymbol{x})$) is a $V-$periodic function of the coordinates $\boldsymbol{x}$. The local bulk and shear moduli are denoted respectively as $\kappa(\boldsymbol{x})$ and $\mu(\boldsymbol{x})$. To determine the overall elastic properties of the material, we need to solve the following periodic boundary value problem for stress $\boldsymbol{\sigma}$ and strain $\boldsymbol{\epsilon}$, where the average of one of these fields over V is given. Then the effective elasticity tensor $\mathbb{C}^e$ can be computed from the linear relation between the average strain $\boldsymbol{E}$ and stress $\boldsymbol{\Sigma}$

$$\boldsymbol{\Sigma} = \mathbb{C}^e\boldsymbol{E}, \quad \boldsymbol{\Sigma} = \langle\boldsymbol{\sigma}\rangle_V, \quad \boldsymbol{E} = \langle\boldsymbol{\epsilon}\rangle_V. \tag{27}$$

Here, we adopt the notation $\langle\rangle_V$ to refer to the average over volume V of the quantity inside the brackets. Introducing a reference material with an isotropic stiffness $\mathbb{C}^0$ (compliance $\mathbb{S}^0$), we have

$$\boldsymbol{\sigma} = \mathbb{C}^0\boldsymbol{\epsilon} + \boldsymbol{\tau}, \quad \boldsymbol{\epsilon} = \mathbb{S}^0\boldsymbol{\sigma} + \boldsymbol{e}, \tag{28}$$

where the eigenstress $\boldsymbol{\tau}$ and the eigenstrain $\boldsymbol{e}$ have been introduced. By usual ways (Milton, 2002; Nemat-Nasser et al., 1982), the integral equation for the eigenstress $\boldsymbol{\tau}$ may be expressed as:

$$\boldsymbol{\tau} = \delta'\mathbb{C}(\boldsymbol{E} - \boldsymbol{\Gamma}^0 * \boldsymbol{\tau}), \quad \delta'\mathbb{C}(\boldsymbol{x}) = \mathbb{C}(\boldsymbol{x}) - \mathbb{C}^0 \tag{29}$$

and the dual integral equation for the eigenstrain $\boldsymbol{e}$

$$\boldsymbol{e} = \delta'\mathbb{S}(\boldsymbol{\Sigma} - \boldsymbol{\Delta}^0 * \boldsymbol{e}), \quad \delta'\mathbb{S}(\boldsymbol{x}) = \mathbb{S}(\boldsymbol{x}) - \mathbb{S}^0. \tag{30}$$

The Green operators $\boldsymbol{\Gamma}^0$ and $\boldsymbol{\Delta}^0$ for strain and stress are defined in Fourier space by:

$$\begin{aligned}
\boldsymbol{\Gamma}^0(\boldsymbol{\xi}) &= \frac{3}{3\kappa_0 + 4\mu_0}\mathbb{E}_2 + \frac{1}{2\mu_0}\mathbb{E}_4 \quad \forall \boldsymbol{\xi} \neq \boldsymbol{0}, \quad \boldsymbol{\Gamma}^0(\boldsymbol{0}) = \boldsymbol{0}, \\
\boldsymbol{\Delta}^0(\boldsymbol{\xi}) &= \frac{18\mu_0\kappa_0}{3\kappa_0 + 4\mu_0}\mathbb{E}_1 + 2\mu_0\mathbb{E}_3 \quad \forall \boldsymbol{\xi} \neq \boldsymbol{0}, \quad \boldsymbol{\Delta}^0(\boldsymbol{0}) = \boldsymbol{0},
\end{aligned} \tag{31}$$

where $\boldsymbol{\xi}$ is the wave vector and the tensors $\mathbb{E}_i$ are defined in Fourier space from the Walpole base by using $\bar{\boldsymbol{\xi}}$ as the unit vector in the direction of $\boldsymbol{\xi}$. The elastic constants κ_0 and μ_0 appearing in (31) are respectively the bulk modulus and the shear modulus associated to the reference tensor $\mathbb{C}^0$. It is clear that the two Eqs. (29) and (30) are equivalent to strain and stress integral equations which Fast Fourier Transform (FFT) numerical homogenization methods are essentially based on (see Appendix A). They also have the same form as (7) and can be solved using Neumann series expansion (or iterative scheme techniques) based on (8,9).

In general, the solutions for strain and stress are unique and independent from the choice of the reference medium. However, the reference material can affect the convergence if Neumann series expansion is used, especially when one of the constituents is chosen as a reference material. From another point of view, the choice of one of the constituents as a reference material simplifies drastically the form of the Neumann series associated to the integral equation. Connections to important statistical information like structure factors appear directly and naturally using this formulation, as it will be shown thereafter. Therefore, instead of using stress or strain formulation, our strategy is to derive a unified formulation by exploiting the relations between stress $\boldsymbol{\sigma}$, strain $\boldsymbol{\epsilon}$ and eigen-stress $\boldsymbol{\tau}$ (or eigen-strain $\boldsymbol{e}$). The two latter quantities are connected via the relation $\boldsymbol{\tau} = -\mathbb{C}^0\boldsymbol{e}$. It will be shown thereafter that this strategy is compatible with the choice of one of the constituents as a reference material.

From the two elementary integral equations, we can construct a family of integral equations for $\boldsymbol{\tau}$ (or $\boldsymbol{e}$ equivalently) by linear combination. Using two tensors $\mathbb{L}(\boldsymbol{x})$ and $\mathbb{I} - \mathbb{L}(\boldsymbol{x})$, we can obtain

$$\boldsymbol{\tau} = \mathbb{A}'\boldsymbol{E} + \mathbb{B}' * \boldsymbol{\tau}, \tag{32}$$

in which

$$\begin{aligned}
\mathbb{A}' &= ((\mathbb{I} - \mathbb{L})(\delta'\mathbb{C}) - \mathbb{L}\mathbb{C}^0(\delta'\mathbb{S})\mathbb{C}^e) \\
\mathbb{B}' &= -((\mathbb{I} - \mathbb{L})(\delta'\mathbb{C})\mathbb{S}^0\mathbb{P} + \mathbb{L}\mathbb{C}^0(\delta'\mathbb{S})\mathbb{Q}).
\end{aligned} \tag{33}$$

Here, the two projection operators $\mathbb{P}$ and $\mathbb{Q}$ are defined again in Fourier space by:

$$\begin{aligned}
\mathbb{P} &= \mathbb{C}^0\boldsymbol{\Gamma}^0 = \mathbb{E}_2 + \mathbb{E}_4 + \frac{3\kappa_0 - 2\mu_0}{3\kappa_0 + 4\mu_0}\mathbb{E}_6, \\
\mathbb{Q} &= \boldsymbol{\Delta}^0\mathbb{S}^0 = \mathbb{E}_1 + \mathbb{E}_3 - \frac{3\kappa_0 - 2\mu_0}{3\kappa_0 + 4\mu_0}\mathbb{E}_6,
\end{aligned} \tag{34}$$

Eq. (32) can be used to solve $\boldsymbol{\tau}$ with an iteration scheme corresponding to the associated Neumann series as long as $\rho(\mathbb{B}') < 1$. This condition guarantees that the Neumann series, which is obtained by repeating the recurrence (32)

$$\begin{aligned}
\boldsymbol{\tau} &= \mathbb{A}'\boldsymbol{E} + \mathbb{B}' * \boldsymbol{\tau} = \mathbb{A}'\boldsymbol{E} + \mathbb{B}' * \mathbb{A}'\boldsymbol{E} + \mathbb{B}' * \mathbb{B}' * \boldsymbol{\tau} \\
&= \ldots = \sum_{n=0}^{\infty} (\mathbb{B}'*)^n \mathbb{A}'\boldsymbol{E}
\end{aligned} \tag{35}$$

will surely converge. The convergence rate depends on the magnitude of $\rho(\mathbb{B}')$. The smaller it is, the faster the series converges. For convenience, let us call the series associated to (29) as $\boldsymbol{E}-$series (ES) and (30) as $\boldsymbol{\Sigma}-$series (SS). Those are particular cases of (32) where $\mathbb{L} = 0$ and $\mathbb{L} = \mathbb{I}$. The series in the form (32) with suitable $\mathbb{L}$ that yields the fastest convergence rate will be called as optimized series and studied in the following.

We consider a two-phase material composed of inclusions embedded in the matrix. At this stage, it can be remarked that the choice of the reference material is crucial in the expression of the power of $\mathbb{B}'$ in (3.1). Indeed, if the reference material is not chosen properly, the operator $\mathbb{B}'$ will contain simultaneously the characteristic functions of both constituents defined thereafter and the expression of $(\mathbb{B}'*)^n$ will become increasingly complicate. Therefore, in the following, the reference material is chosen to be the matrix $\mathbb{C}^0$ and the stiffness of the inclusion is denoted as $\mathbb{C}^1$. The tensor $\mathbb{L}$ is assumed to be constant and isotropic with the representation

$$\mathbb{L} = 2\alpha\mathbb{K} + 3\beta\mathbb{J} \tag{36}$$

in which α and β are two constants. Like $\mathbb{L}$, the tensor $\mathbb{C}^i$ with $i = 0, 1$ can be expressed in a similar way using the bulk stiffness κ_i and the shear stiffness μ_i as parameters.

3.2. Optimization based on the Green operators

In this section, we employ the method developed in Nguyen et al. (2016) and Milton (2002) for heat conduction to estimate the convergence rate of the general series (32) in elasticity. This method will require the mathematical preliminaries that we presented previously. Adopting the notation χ for the characteristic function,

$$\chi(\boldsymbol{x}) = 0 \quad \text{in matrix}, \quad \chi(\boldsymbol{x}) = 1 \quad \text{in inclusion} \tag{37}$$

and recalling that the reference tensor is the elasticity tensor of the matrix, we can rewrite the Neumann series in the following form

$$\boldsymbol{\tau} = \sum_{j=0}^{\infty} (\mathbb{B}')^{*j}\mathbb{A}'\boldsymbol{E} \tag{38}$$

where $\mathbb{A}' = \chi\mathbb{A}, \quad \mathbb{B}' = \chi\mathbb{B}$ and

$$\begin{aligned}
\mathbb{A} &= ((\mathbb{I} - \mathbb{L})(\delta\mathbb{C}) - \mathbb{L}\mathbb{C}^0(\delta\mathbb{S})\mathbb{C}^e) \\
\mathbb{B} &= -((\mathbb{I} - \mathbb{L})(\delta\mathbb{C})\mathbb{S}^0\mathbb{P} + \mathbb{L}\mathbb{C}^0(\delta\mathbb{S})\mathbb{Q}) \\
\delta\mathbb{C} &= \mathbb{C}^1 - \mathbb{C}^0, \quad \delta\mathbb{S} = \mathbb{S}^1 - \mathbb{S}^0
\end{aligned} \tag{39}$$

It is noteworthy that the choice of the matrix as a reference material allows us to obtain an expression involving only χ in its expression and power series, while another choice would contain two characteristic functions of the two materials at the same time.

Another strategy behind this expression is also that it is easier to quantify separately the spectral radius and norm of $\mathbb{B}$ and χ, which in turn provides information on $\mathbb{B}'$. The function χ takes only 0 and 1 values and depends on the distribution of the inclusions in the cell. Its spectral radius and norm can be obtained straightforwardly, for example

$$\rho(\chi) = \|\chi\| = 1. \tag{40}$$

Intuitively, to optimize the convergence rate of $\mathbb{B}'$, we need to optimize $\rho(\mathbb{B})$ or the norm $\|\mathbb{B}\|$. Since $\mathbb{B}$ is generally not self-adjoint, optimizing $\|\mathbb{B}\|$ and $\rho(\mathbb{B})$ with $\mathbb{L}$ may lead to different results (see Figs. 1 and 2). For the sake of clarity, we shall use the two abbreviated names: OR for optimization by spectral radius and ON for optimization by norm.

As an example, let us consider the case where the two materials are isotropic with the same Poisson ratio ν, or

$$\mathbb{C}^1 = \varepsilon\mathbb{C}^0, \tag{41}$$

where ε is the contrast ratio. We are also limited to the case where

$$\mathbb{L} = 2\alpha\mathbb{I}, \tag{42}$$

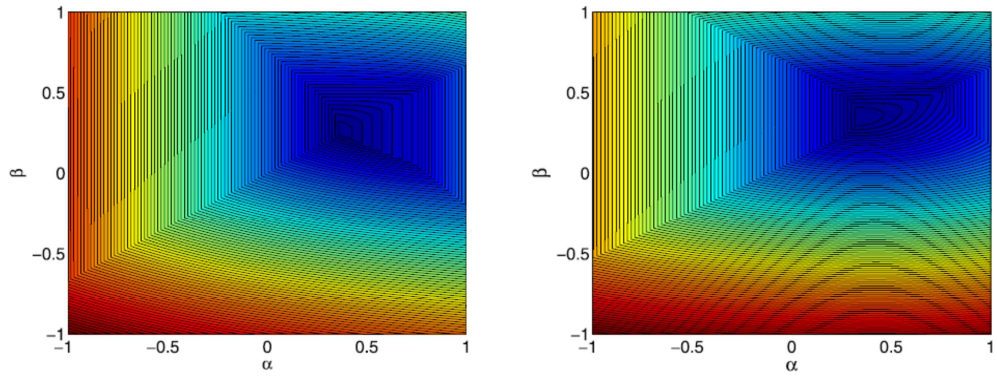

Fig. 1. Isolines of spectral radius $\rho(\mathbb{B})$ (left) and norm $\|\mathbb{B}\|$ (right) as functions of α and β. The results are obtained for the case where the two materials are of the same Poisson ratio $\nu = 0.3$ and stiffness ratio $\varepsilon = 3$. The optimal values by the two methods are respectively $(\alpha, \beta) = (0.375, 0.250)$ and $(\alpha, \beta) = (0.338, 0.349)$.

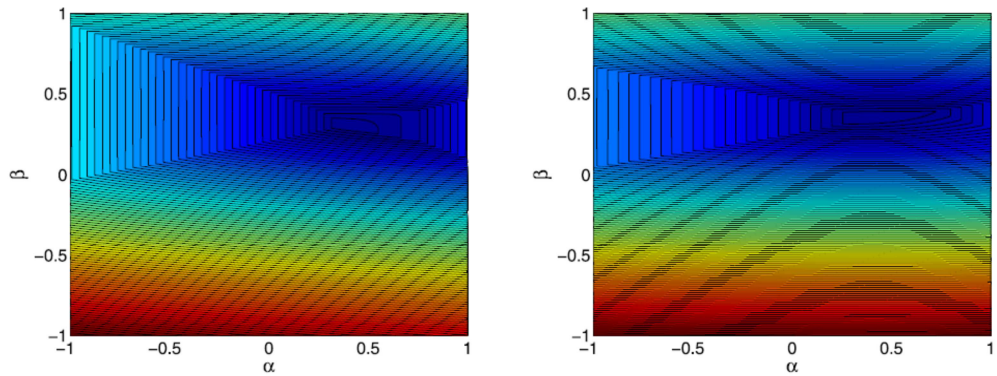

Fig. 2. Isolines of spectral radius $\rho(\mathbb{B})$ (left) and norm $\|\mathbb{B}\|$ (right) as functions of α and β. The results are obtained for two materials with the following parameters $\nu_1 = 0.4, \nu_0 = 0.3, \mu_1/\mu_0 = 3$. The optimal values by the two methods are respectively $(\alpha, \beta) = (0.355, 0.298)$ and $(\alpha, \beta) = (0.309, 0.349)$.

and minimize $\rho(\mathbb{B})$. First, $\mathbb{B}$ can be written explicitly as

$$\mathbb{B} = -(\varepsilon-1)(1-2\alpha)(\mathbb{E}_2+\mathbb{E}_4) + 2\alpha\frac{(\varepsilon-1)}{\varepsilon}(\mathbb{E}_1+\mathbb{E}_3) - \frac{3\kappa_0-2\mu_0}{3\kappa_0+4\mu_0}\mathbb{E}_6\left[(1-2\alpha)(\varepsilon-1)+2\alpha\frac{(\varepsilon-1)}{\varepsilon}\right] \tag{43}$$

It is clear that the spectral radius of $\mathbb{B}$ can be evaluated as

$$\rho(\mathbb{B}) = \max\left\{|(\varepsilon-1)(1-2\alpha)|, \left|2\alpha\frac{(\varepsilon-1)}{\varepsilon}\right|\right\}. \tag{44}$$

Since both eigenvalues are linear function of α, optimizing $\rho(\mathbb{B})$ yields the following results

$$2\alpha = \frac{\varepsilon}{\varepsilon+1}, \quad \rho(\mathbb{B}) = \left|\frac{\varepsilon-1}{\varepsilon+1}\right|,$$
$$\mathbb{B} = \frac{\varepsilon-1}{\varepsilon+1}\left(\mathbb{E}_1-\mathbb{E}_2+\mathbb{E}_3-\mathbb{E}_4-\frac{2(3\kappa_0-2\mu_0)}{3\kappa_0+4\mu_0}\mathbb{E}_6\right). \tag{45}$$

Comparing with two original series, for example the ES series

$$\mathbb{B} = -(\varepsilon-1)\left(\mathbb{E}_2+\mathbb{E}_4+\frac{3\kappa_0-2\mu_0}{3\kappa_0+4\mu_0}\mathbb{E}_6\right), \quad \rho(\mathbb{B}) = |\varepsilon-1|, \tag{46}$$

and the SS series

$$\mathbb{B} = -\frac{1-\varepsilon}{\varepsilon}\left(\mathbb{E}_1+\mathbb{E}_3-\frac{3\kappa_0-2\mu_0}{3\kappa_0+4\mu_0}\mathbb{E}_6\right), \quad \rho(\mathbb{B}) = \left|\frac{\varepsilon-1}{\varepsilon}\right|, \tag{47}$$

the series after optimization shows a clear advantage. The spectral radius of the latter is the smallest and less than 1. The ES series can diverge if $\varepsilon > 2$ and the SS series can diverge if $\varepsilon < 1/2$.

Minimizing $\rho(\mathbb{B})$ and $\|\mathbb{B}\|$ for the general case is not analytically simple, but it can be done numerically without difficulties. The main problem is that we need to ensure the convergence related to operator $\rho(\mathbb{B}')$. However, optimizing $\rho(\mathbb{B})$ only guarantees the convergence of the series associated to $\mathbb{B}$ not $\mathbb{B}'$ while optimizing $\|\mathbb{B}\|$ may overestimate $\rho(\mathbb{B}')$. This is due to the inequalities

$$\rho(\mathbb{B}') \le \|\mathbb{B}'\|, \quad \rho(\mathbb{B}) \le \|\mathbb{B}\|, \quad \|\mathbb{B}'\| \le \|\chi\|\|\mathbb{B}\| = \|\mathbb{B}\|. \tag{48}$$

As a result, in the case where $\mathbb{B}$ is not self-adjoint, those estimations may not be strict enough. To overcome those issues, we shall present now a more direct optimization method (OD) to estimate $\rho(\mathbb{B}')$, detailed in the next subsection.

3.3. Direct estimation of $\rho(\mathbb{B}')$ and optimization

We introduce now an approach which is closely related to the one presented by Michel et al. (1999) to estimate the convergence rate of the series. We begin first with the ES series whose eigenequation reads

$$-(\mathbb{C}-\mathbb{C}^0)\mathbb{S}^0\mathbb{P}*\boldsymbol{\tau} = \lambda\boldsymbol{\tau}. \tag{49}$$

Equivalently, we can rewrite the above equation as

$$-\left(\mathbb{C}'-\mathbb{C}^0\right)\mathbb{S}^0\mathbb{P}*\boldsymbol{\tau} = \boldsymbol{\tau}, \quad \mathbb{C}' = \frac{1}{\lambda}\mathbb{C} - \frac{(1-\lambda)}{\lambda}\mathbb{C}^0. \tag{50}$$

Comparing with (29), we conclude that this is the equation for the boundary value problem with zero strain $\boldsymbol{E} = 0$ and local stiffness $\mathbb{C}'$. Since there exists a non-trivial solution $\boldsymbol{\tau}$, the local stiffness $\mathbb{C}'$

of the imaginary material can not be either negative definite (notation $\prec 0$) or positive definite (notation $\succ 0$) for the whole physical space, or equivalently

$$\exists \boldsymbol{x} \,|\, \mathbb{C}(\boldsymbol{x}) - (1-\lambda)\mathbb{C}^0 \not\succ 0, \quad \exists \boldsymbol{x} \,|\, \mathbb{C}(\boldsymbol{x}) - (1-\lambda)\mathbb{C}^0 \not\prec 0. \tag{51}$$

Eq. (51) is identical to the conditions obtained for the basic scheme in Michel et al. (2001) . Hence, similar results can be deduced

$$\begin{aligned} \lambda &\geq \min\left\{\min_{\boldsymbol{x}}\left(1-\frac{\kappa(\boldsymbol{x})}{\kappa_0}\right), \min_{\boldsymbol{x}}\left(1-\frac{\mu(\boldsymbol{x})}{\mu_0}\right)\right\}, \\ \lambda &\leq \max\left\{\max_{\boldsymbol{x}}\left(1-\frac{\kappa(\boldsymbol{x})}{\kappa_0}\right), \max_{\boldsymbol{x}}\left(1-\frac{\mu(\boldsymbol{x})}{\mu_0}\right)\right\}. \end{aligned} \tag{52}$$

For a two phase material with the same Poisson ratio in both phases $\mathbb{C}^1 = \varepsilon\mathbb{C}^0$, we can deduce that

$$|\lambda| \leq |1-\varepsilon|. \tag{53}$$

It is clear that for high contrast ratios, for example $\varepsilon > 2$, we can not guarantee the convergence of the series. In this case, the convergence of the series can only be achieved by using another reference material than the one of the matrix.

Analogously, considering the SS series with the eigen equation

$$-\mathbb{C}^0(\mathbb{S}-\mathbb{S}^0)\mathbb{Q} * \boldsymbol{\tau} = \lambda\boldsymbol{\tau}, \tag{54}$$

we can show that $\boldsymbol{\tau}$ is the solution of the new boundary value problem with local compliance $\mathbb{S}'$ and zero stress $\boldsymbol{\Sigma} = 0$, namely

$$-\mathbb{C}^0\big(\mathbb{S}'-\mathbb{S}^0\big)\mathbb{Q} * \boldsymbol{\tau} = \boldsymbol{\tau}, \quad \mathbb{S}' = \frac{1}{\lambda}\mathbb{S} - \frac{(1-\lambda)}{\lambda}\mathbb{S}^0. \tag{55}$$

As a result, we can deduce the similar condition for λ

$$|\lambda| \leq \left|1-\varepsilon^{-1}\right|, \tag{56}$$

which means that the SS series can diverge at small contrast ratio, say $\varepsilon < 1/2$.

Considering the general series, we shall bound the eigenvalue λ issued from the equation

$$-(\mathbb{I}-\mathbb{L})(\mathbb{C}-\mathbb{C}^0)\mathbb{S}^0\mathbb{P} * \boldsymbol{\tau} - \mathbb{L}\mathbb{C}^0(\mathbb{S}-\mathbb{S}^0)\mathbb{Q} * \boldsymbol{\tau} = \lambda\boldsymbol{\tau}. \tag{57}$$

Like for the two previous cases, our strategy is to find the imaginary material that admits non-trivial solution $\boldsymbol{\tau}$ with zero average strain $\boldsymbol{E} = 0$ and stress $\boldsymbol{\Sigma} = 0$. Our technique is to assume that the relations

$$\begin{aligned} -\frac{1}{\lambda}(\mathbb{I}-\mathbb{L})(\mathbb{C}-\mathbb{C}^0)\mathbb{S}^0\mathbb{P} * \boldsymbol{\tau} &= \mathbb{M}\boldsymbol{\tau}, \\ -\frac{1}{\lambda}\mathbb{L}\mathbb{C}^0(\mathbb{S}-\mathbb{S}^0)\mathbb{Q} * \boldsymbol{\tau} &= (\mathbb{I}-\mathbb{M})\boldsymbol{\tau}, \end{aligned} \tag{58}$$

hold true at the same time and compute the corresponding isotropic tensor $\mathbb{M}(\boldsymbol{x})$. In order to do that, we have to rearrange (58) in the following way

$$-(\mathbb{C}'-\mathbb{C}^0)\mathbb{S}^0\mathbb{P} * \boldsymbol{\tau} = \boldsymbol{\tau}, \quad -\mathbb{C}^0(\mathbb{S}'-\mathbb{S}^0)\mathbb{Q} * \boldsymbol{\tau} = \boldsymbol{\tau} \tag{59}$$

where $\mathbb{C}'$ and $\mathbb{S}'$ are the stiffness and compliance tensors

$$\begin{aligned} \mathbb{C}' &= \frac{1}{\lambda}\mathbb{M}^{-1}(\mathbb{I}-\mathbb{L})(\mathbb{C}-\mathbb{C}^0) + \mathbb{C}^0 \\ \mathbb{S}' &= \frac{1}{\lambda}\mathbb{S}^0(\mathbb{I}-\mathbb{M})^{-1}\mathbb{L}\mathbb{C}^0(\mathbb{S}-\mathbb{S}^0) + \mathbb{S}^0. \end{aligned} \tag{60}$$

The next step is to choose suitably $\mathbb{M}$ so that $\mathbb{C}'$ and $\mathbb{S}'$ are compatible, meaning that they are stiffness and compliance of the same imaginary material

$$\mathbb{C}'(\boldsymbol{x})\mathbb{S}'(\boldsymbol{x}) = \mathbb{I}, \quad \forall \boldsymbol{x}. \tag{61}$$

This choice will guarantee that $\boldsymbol{\tau}$ corresponds to the same boundary value problem. As a consequence, $\boldsymbol{\tau}$ satisfies automatically both constraints (59) at the same time. It is clear that if $\boldsymbol{x}$ belongs to the matrix, this condition is automatically verified because

$$\mathbb{C}'(\boldsymbol{x}) = \mathbb{C}^0 \succ 0, \quad \mathbb{S}'(\boldsymbol{x}) = \mathbb{S}^0 \succ 0. \tag{62}$$

The compatibility condition can be recast in the form

$$\left[\frac{1}{\lambda}\mathbb{M}^{-1}(\mathbb{I}-\mathbb{L})(\delta\mathbb{C})\mathbb{S}^0 + \mathbb{I}\right]\left[\frac{1}{\lambda}(\mathbb{I}-\mathbb{M})^{-1}\mathbb{L}\mathbb{C}^0(\delta\mathbb{S}) + \mathbb{I}\right] = \mathbb{I}. \tag{63}$$

After finding $\mathbb{M}$ from (63), it is sufficient to bound λ via the positive-definite and negative definite properties of $\mathbb{C}'$ and $\mathbb{S}'$ as before. Due to the fact that $\mathbb{C}'$ and $\mathbb{S}'$ are already positive definite in the matrix (62), those quantites can not be positive definite in the inclusion

$$\frac{1}{\lambda}\mathbb{M}^{-1}(\mathbb{I}-\mathbb{L})(\delta\mathbb{C}) + \mathbb{C}^0 \not\succ 0. \tag{64}$$

Since (63) involves isotropic tensors, it is better to use a decomposition based on orthogonal tensors $\mathbb{J}$ and $\mathbb{K}$. Assuming that

$$\mathbb{M} = 3\beta'\mathbb{J} + 2\alpha'\mathbb{K} \tag{65}$$

and posing $\varepsilon_m = \mu_1/\mu_0$ and $\varepsilon_k = \kappa_1/\kappa_0$, the corresponding equation for α', β' reads

$$\begin{aligned} \left((1-2\alpha)\frac{(\varepsilon_m-1)}{2\lambda\alpha'}+1\right)\left(1-2\alpha\frac{(\varepsilon_m-1)}{\varepsilon_m\lambda(1-2\alpha')}\right) &= 1, \\ \left((1-3\beta)\frac{(\varepsilon_k-1)}{3\lambda\beta'}+1\right)\left(1-3\beta\frac{(\varepsilon_k-1)}{\varepsilon_k\lambda(1-3\beta')}\right) &= 1. \end{aligned} \tag{66}$$

Solving (66) for α', β' yields the solution

$$\begin{aligned} 2\alpha' &= \frac{\varepsilon_m\lambda(1-2\alpha) - 2\alpha(1-2\alpha)(\varepsilon_m-1)}{[(1-2\alpha)\varepsilon_m + 2\alpha]\lambda}, \\ 3\beta' &= \frac{\varepsilon_k\lambda(1-3\beta) - 3\beta(1-3\beta)(\varepsilon_m-1)}{[(1-3\beta)\varepsilon_m + 3\beta]\lambda}. \end{aligned} \tag{67}$$

Substituting α', β' back to (64), we obtain the condition

$$\frac{2\alpha(\varepsilon_m-1)/\varepsilon_m - \lambda}{(1-2\alpha)(\varepsilon_m-1)+\lambda} \geq 0, \quad \text{or} \quad \frac{3\beta(\varepsilon_k-1)/\varepsilon_k - \lambda}{(1-3\beta)(\varepsilon_k-1)+\lambda} \geq 0. \tag{68}$$

In any case, we must have the inequalities

$$\begin{aligned} &|\lambda| \leq \max\{|(1-2\alpha)(\varepsilon_m-1)|, |2\alpha(\varepsilon_m-1)/\varepsilon_m|\} \\ &\text{or} \quad |\lambda| \leq \max\{|(1-3\beta)(\varepsilon_k-1)|, |3\beta(\varepsilon_k-1)/\varepsilon_k|\} \end{aligned} \tag{69}$$

which bound the spectral radius of the general operators. To optimize the acceptable value of $|\lambda|$, one must have

$$2\alpha = \varepsilon_m/(\varepsilon_m+1), \quad 3\beta = \varepsilon_k/(\varepsilon_k+1), \tag{70}$$

so that we can obtain the inequalities

$$|\lambda| \leq \max\left\{\left|\frac{\varepsilon_m-1}{\varepsilon_m+1}\right|, \left|\frac{\varepsilon_k-1}{\varepsilon_k+1}\right|\right\}, \tag{71}$$

which guarantees the convergence of the series for any finite contrast. Having derived the optimal values of α and β, we can write explicitly the expressions for $\mathbb{A}$ and $\mathbb{B}$ as follows

$$\begin{aligned} \mathbb{A} &= \left[\left(3\frac{\varepsilon_k-1}{\varepsilon_k+1}\kappa_0\mathbb{J} + 2\frac{\varepsilon_m-1}{\varepsilon_m+1}\mu_0\mathbb{K}\right) + \left(\frac{\varepsilon_k-1}{\varepsilon_k+1}\mathbb{J} + \frac{\varepsilon_m-1}{\varepsilon_m+1}\mathbb{K}\right)\mathbb{C}^e\right], \\ \mathbb{B} &= \left(\frac{\varepsilon_k-1}{\varepsilon_k+1}\mathbb{J} + \frac{\varepsilon_m-1}{\varepsilon_m+1}\mathbb{K}\right)\left(\mathbb{E}_1 - \mathbb{E}_2 + \mathbb{E}_3 - \mathbb{E}_4 - \frac{2(3\kappa_0-2\mu_0)}{3\kappa_0+4\mu_0}\mathbb{E}_6\right). \end{aligned} \tag{72}$$

To differentiate from the ON and OR series obtained by different optimization methods, the series issued from (72) will be associated to the notation OD (optimization by direct method). Table 1 shows numerical examples corresponding to the three methods of optimization. Taking the properties of the constituents as input,

Table 1
Comparison of the results α, β issued from three methods of optimization. Notations: OR for optimization based on spectral radius of $\mathbb{B}$, ON for optimization based on norm of $\mathbb{B}$ and OD for optimization based on the direct estimation of spectral radius of $\mathbb{B}'$.

Case	α			β		
	OR	ON	OD	OR	ON	OD
$\nu_1 = \nu_0 = 0.3$ $\mu_1/\mu_0 = 0.01$	0.0040	−0.0031	0.0050	0.0027	−0.0012	0.0033
$\nu_1 = 0.1, \nu_0 = 0.3$ $\mu_1/\mu_0 = 0.1$	0.0525	−0.0215	0.0528	0.0430	0.0037	0.0159
$\nu_1 = 0.4, \nu_0 = 0.3$ $\mu_1/\mu_0 = 1$	0.923	−1.000	0.250	0.259	0.353	0.228
$\nu_1 = 0.4, \nu_0 = 0.3$ $\mu_1/\mu_0 = 3$	0.355	0.309	0.375	0.298	0.349	0.289
$\nu_1 = 0.2, \nu_0 = 0.3$ $\mu_1/\mu_0 = 10$	0.455	0.453	0.454	0.281	0.347	0.287
$\nu_1 = 0.1, \nu_0 = 0.3$ $\mu_1/\mu_0 = 100$	0.496	0.496	0.495	0.325	0.337	0.326
$\nu_1 = 0.1, \nu_0 = 0.3$ $\mu_1/\mu_0 = 1000$	0.500	0.500	0.499	0.333	0.334	0.332

one can compute the values α and β in order to minimize the quantities $\|\mathbb{B}\|$ (ON) or $\rho(\mathbb{B})$ (OR) or $\rho(\mathbb{B}')$ (OD). One can remark that the three methods can yield different results. Those differences can have a impact on the estimates presented in the next section. However, it is interesting to note that at the infinite contrast limits, numerical results show that the coefficients α, β tend to the same value (0, 0) for void inclusion and (1/2, 1/3) for rigid inclusion.

3.4. Estimation of the overall elastic properties

To determine the effective stiffness tensor $\mathbb{C}^e$, we need to find the average $\boldsymbol{\tau}$ over the inclusion domain $\langle\boldsymbol{\tau}\rangle_\Omega$. The latter is connected to $\mathbb{C}^e$ via the relation

$$f\langle\boldsymbol{\tau}\rangle_\Omega = (\mathbb{C}^e - \mathbb{C}^0)\boldsymbol{E}. \tag{73}$$

On the other hand, $\langle\boldsymbol{\tau}\rangle_\Omega$ can be obtained by averaging (38), for example

$$\langle\boldsymbol{\tau}\rangle_\Omega = \sum_{j=0}^{\infty} \mathbb{D}^j \mathbb{A}\boldsymbol{E}, \tag{74}$$

in which the tensors $\mathbb{D}^0, \mathbb{D}^1, ..$ are determined with the formulas

$$\begin{aligned}
&\mathbb{D}^0 = \langle(\mathbb{B}\chi)^0\rangle_\Omega = \mathbb{I},\\
&\mathbb{D}^1 = \langle(\mathbb{B}\chi)^1\rangle_\Omega = f^{-1}\sum_{\boldsymbol{\xi}} \chi(-\boldsymbol{\xi})\mathbb{B}(\boldsymbol{\xi})\chi(\boldsymbol{\xi}),\\
&\mathbb{D}^2 = \langle(\mathbb{B}\chi)^2\rangle_\Omega = f^{-1}\sum_{\boldsymbol{\xi}} \chi(-\boldsymbol{\xi})\mathbb{B}(\boldsymbol{\xi})\sum_{\boldsymbol{\xi}'} \chi(\boldsymbol{\xi}-\boldsymbol{\xi}')\mathbb{B}(\boldsymbol{\xi}')\chi(\boldsymbol{\xi}'),\\
&\dots\\
&\mathbb{D}^j = \langle(\mathbb{B}\chi)^j\rangle_\Omega\\
&\quad = f^{-1}\sum_{\boldsymbol{\xi}^1,\boldsymbol{\xi}^2,\dots,\boldsymbol{\xi}^n} \chi(-\boldsymbol{\xi}^1)\chi(\boldsymbol{\xi}^1-\boldsymbol{\xi}^2)\dots\chi(\boldsymbol{\xi}^{j-1}-\boldsymbol{\xi}^j)\chi(\boldsymbol{\xi}^1)\\
&\mathbb{B}(\boldsymbol{\xi}^1)\dots\mathbb{B}(\boldsymbol{\xi}^j).
\end{aligned} \tag{75}$$

Substituting (75) into (74) and (73) yields the expression for $\mathbb{C}^e$

$$\mathbb{C}^e - \mathbb{C}^0 = f\sum_{j=0}^{\infty} \mathbb{D}^j[(\mathbb{I}-\mathbb{L})(\delta\mathbb{C}) - \mathbb{L}\mathbb{C}^0(\delta\mathbb{S})\mathbb{C}^e]. \tag{76}$$

Generally, in numerical applications, we need to truncate the series up-to a sufficiently high value n

$$\mathbb{C}^e \simeq \left[\mathbb{I} + f\sum_{j=0}^{n} \mathbb{D}^j\mathbb{L}\mathbb{C}^0(\delta\mathbb{S})\right]^{-1}\left[\mathbb{I} + f\sum_{j=0}^{n} \mathbb{D}^j(\mathbb{I}-\mathbb{L})(\delta\mathbb{C})\mathbb{S}^0\right]\mathbb{C}^0. \tag{77}$$

The estimate (77), based on truncation, works well if the remainder of the series is negligible. It can be improved by a better treatment of the series (To and Bonnet, 2014; Nguyen et al., 2016). Indeed, repeating the recurrence at step n we obtain an equation for $\boldsymbol{\tau}$

$$\boldsymbol{\tau} = \chi\sum_{j=0}^{n-1}(\mathbb{B}\chi)^j\mathbb{A} + (\chi\mathbb{B})^n\boldsymbol{\tau}. \tag{78}$$

Averaging both sides over the inclusion volume and making the approximation

$$\boldsymbol{\tau} \simeq \chi\langle\boldsymbol{\tau}\rangle_\Omega, \tag{79}$$

we obtain the following equation for $\langle\boldsymbol{\tau}\rangle_\Omega$

$$\langle\boldsymbol{\tau}\rangle_\Omega \simeq \sum_{j=0}^{n-1}\mathbb{D}^j\mathbb{A}\boldsymbol{E} + \mathbb{D}^n\langle\boldsymbol{\tau}\rangle_\Omega. \tag{80}$$

Solving (80) for $\langle\boldsymbol{\tau}\rangle_\Omega$ and substituting back into (73), we obtain a new expression for $\mathbb{C}^e$

$$\begin{aligned}
\mathbb{C}^e \simeq &\left[(\mathbb{I}-\mathbb{D}^n) + f\sum_{j=0}^{n-1}\mathbb{D}^j\mathbb{L}\mathbb{C}^0(\delta\mathbb{S})\right]^{-1}\\
&\left[(\mathbb{I}-\mathbb{D}^n) + f\sum_{j=0}^{n-1}\mathbb{D}^j(\mathbb{I}-\mathbb{L})(\delta\mathbb{C})\mathbb{S}^0\right]\mathbb{C}^0.
\end{aligned} \tag{81}$$

In the case where the effective material is isotropic or at least cubic, we can extract the main shear modulus μ_e and the bulk modulus κ_e using the expressions

$$\begin{aligned}
&\frac{\mu_e}{\mu_0} \simeq 1 + f\frac{(1-2\alpha)\delta\mu/\mu_0 + 2\alpha\delta\mu/\mu_1}{\frac{1-2\alpha_n}{\sum_{j=0}^{n-1}2\alpha_j} - 2\alpha f\delta\mu/\mu_1}\\
&\frac{\kappa_e}{\kappa_0} \simeq 1 + f\frac{(1-3\beta)\delta\kappa/\kappa_0 + 3\beta\delta\kappa/\kappa_1}{\frac{1-3\beta_n}{\sum_{j=0}^{n-1}3\beta_j} - 3\beta f\delta\kappa/\kappa_1},\\
&\mu_e = C^e_{1212}, \quad 3\kappa_e = C^e_{1111} + 2C^e_{1122},\\
&\alpha_j = D^j_{1212}, \quad 3\beta_j = D^j_{1111} + 2D^j_{1122},
\end{aligned} \tag{82}$$

From (82), it is interesting to remark that all the microstructure information is contained in the parameters $\frac{1-2\alpha_n}{\sum_{j=0}^{n-1}2\alpha_j}$ and $\frac{1-3\beta_n}{\sum_{j=0}^{n-1}3\beta_j}$.

3.5. Distributions of non overlapping spheres

We assume now that the unit cell V of dimensions $l \times l \times l$ contains N identical non overlapping spheres of radius R. The shape

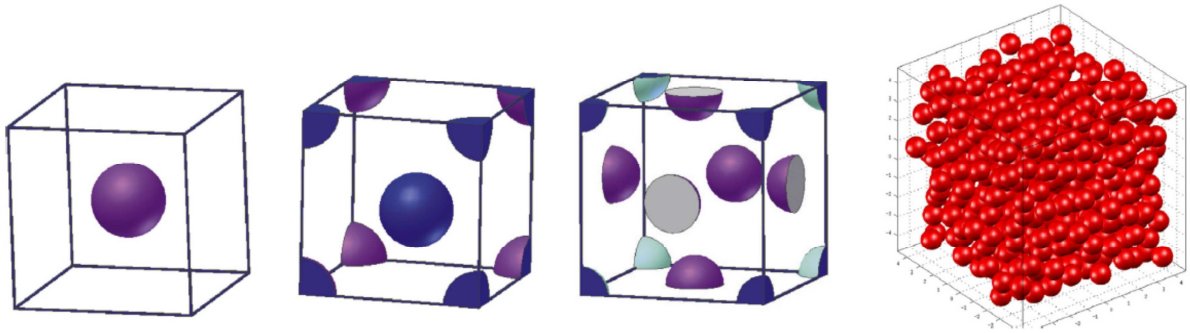

Fig. 3. Different arrangements of non-overalapping spheres in cubic unit cell. From left to right: simple cubic (SC), body centered cubic (BCC), face centered cubic (FCC) and random distribution (RD). The random distribution is generated by Event Driven Molecular Dynamics method.

functions $\chi(\boldsymbol{\xi})$ become

$$\chi(\boldsymbol{\xi}) = \frac{V_s}{V} F(\boldsymbol{\xi})\rho(\boldsymbol{\xi}), \quad \rho(\boldsymbol{\xi}) = \sum_{i=1}^{N} e^{-i\boldsymbol{\xi}.\boldsymbol{x}_i}, \tag{83}$$

where $\boldsymbol{x}_i$ is the center location of the inclusion numbered i in the cell. The form factor $F(\boldsymbol{\xi})$ and inclusion volumes V_s admit the following form

$$V_s = \frac{4\pi}{3}R^3, \quad F(\boldsymbol{\xi}) = 3\frac{\sin\eta - \eta\cos\eta}{\eta^3},$$
$$\eta = |\boldsymbol{\eta}|, \quad \eta_i = R\xi_i = 2\pi n_i R/l, \quad i = 1,2,3 \tag{84}$$

For cubic arrangements of spheres (see Fig. 3), the formulas of $\chi(\boldsymbol{\xi})$ are known explicitly (Nemat-Nasser et al., 1982; Bonnet, 2007).

- Simple Cubic (SC)

$$\chi(\boldsymbol{\xi}) = 3f\frac{\sin\eta - \eta\cos\eta}{\eta^3} \tag{85}$$

- Body Centered Cubic (BC)

$$\chi(\boldsymbol{\xi}) = \frac{3f}{2}\frac{\sin\eta - \eta\cos\eta}{\eta^3}[1 + (-1)^{n_1+n_2+n_3}] \tag{86}$$

- Face Centered Cubic (FCC)

$$\chi(\boldsymbol{\xi}) = \frac{3f}{4}\frac{\sin\eta - \eta\cos\eta}{\eta^3}[(-1)^{n_1} + (-1)^{n_2} + (-1)^{n_3} + (-1)^{n_1+n_2+n_3}] \tag{87}$$

Using these expressions, we can compute numerically the intermediate tensors $\mathbb{D}^n$ at any order n (see Appendix B). The first order tensor $\mathbb{D}^1$ can be expressed more explicitly and related to Hashin–Shtrikman estimates, as shown in the next subsection.

3.5.1. Computation of the intermediate tensor $\mathbb{D}^1$ and first order estimates

It is possible to derive analytically expressions for the first two tensors $\mathbb{D}^0 = \mathbb{I}$ (or $2\alpha_0 = 1$ and $3\beta_0 = 1$) and $\mathbb{D}^1$ (To et al., 2016) which is a lattice sum. In the case where $\mathbb{D}^1$ is a cubic tensor, we can compute explicitly the coefficients β_1 and α_1 associated to $\mathbb{D}^1$

$$2\alpha_1 = -\left[(1-2\alpha)\frac{\delta\mu}{\mu_0}\left(\frac{2}{3}(1-f) - S_3\frac{4(3\kappa_0+\mu_0)}{3\kappa_0+4\mu_0}\right) - 2\alpha\frac{\delta\mu}{\mu_1}\left(\frac{1}{3}(1-f) + S_3\frac{4(3\kappa_0+\mu_0)}{3\kappa_0+4\mu_0}\right)\right],$$
$$3\beta_1 = -(1-f)\left[(1-3\beta)\frac{\delta\kappa}{\kappa_0}\frac{3\kappa_0}{3\kappa_0+4\mu_0} - 3\beta\frac{\delta\kappa}{\kappa_1}\frac{4\mu_0}{3\kappa_0+4\mu_0}\right] \tag{88}$$

via the lattice sums S_1, S_2 and S_3 defined as

$$S_1 = f^{-1}\sum_{\boldsymbol{\xi}} \bar{\xi}_i^2 \chi(\boldsymbol{\xi})\chi(-\boldsymbol{\xi}), \quad i = 1,2,3$$
$$S_2 = f^{-1}\sum_{\boldsymbol{\xi}} \bar{\xi}_i^4 \chi(\boldsymbol{\xi})\chi(-\boldsymbol{\xi}), \quad i = 1,2,3$$
$$S_3 = f^{-1}\sum_{\boldsymbol{\xi}} \bar{\xi}_i^2\bar{\xi}_j^2 \chi(\boldsymbol{\xi})\chi(-\boldsymbol{\xi}), \quad i,j = 1,2,3, \quad i \neq j \tag{89}$$

Expression (88) has been obtained by making use of the additional identities

$$S_1 = (1-f)/3, \quad S_2 + 2S_3 = S_1 \tag{90}$$

and some intermediate results in Appendix B. Substituting $n = 1$ and β_1 in (88) into (82) and making use of $2\alpha_0 = 1$ and $3\beta_0 = 1$, we can recover the Hashin–Shtrikman (HS) estimate for κ_e regardless the chosen values of α and β

$$\frac{\kappa_e}{\kappa_0} = 1 + \frac{f}{\frac{\kappa_0}{\delta\kappa} + (1-f)\frac{3\kappa_0}{3\kappa_0+4\mu_0}} \tag{91}$$

Analogously, all the estimates of μ_e are reduced at order 1 to

$$\frac{\mu_e}{\mu_0} = 1 + \frac{f}{\frac{\mu_0}{\delta\mu} + \frac{2}{3}(1-f) - 4S_3\frac{3\kappa_0+\mu_0}{3\kappa_0+4\mu_0}} \tag{92}$$

where the lattice sum S_3 can be evaluated by semi-analytical expressions (To et al., 2016). We will show later that in the case of an isotropic random distribution, this first order estimate of μ_e is identical to HS estimate.

For higher orders $n \geq 2$, numerical summation can be used to compute $\mathbb{D}^n$ which in turn provides better estimates of κ_e and μ_e.

3.6. Random distributions of non overlapping spheres and relation with structure factors

Regarding random distribution (RD) in Fig. 3, we adopt the ergodicity hypothesis implying that at the infinite volume limit (both N and $V \to \infty$), the tensors $\mathbb{D}^j$ are identical to their ensemble average, both being denoted by $\langle\ldots\rangle$. As a result, we obtain now statistical relations

$$\mathbb{D}^1 = \frac{V_s}{V}\sum_{\boldsymbol{\xi}} F(\boldsymbol{\xi})F(-\boldsymbol{\xi})\mathbb{B}(\boldsymbol{\xi})S^{(2)}(\boldsymbol{\xi})$$
$$\mathbb{D}^2 = \frac{V_s^2}{V^2}\sum_{\boldsymbol{\xi},\boldsymbol{\xi}'} F(\boldsymbol{\xi})F(\boldsymbol{\xi}')F(\boldsymbol{\xi}-\boldsymbol{\xi}')\mathbb{B}(\boldsymbol{\xi})\mathbb{B}(\boldsymbol{\xi}')S^{(3)}(-\boldsymbol{\xi},\boldsymbol{\xi}'), \quad \text{etc.} \tag{93}$$

with $S^{(2)}$, $S^{(3)}$ being the structure factor and the triplet structure factor given by

$$S^{(2)}(\boldsymbol{\xi}) = \frac{1}{N}\langle \rho(\boldsymbol{\xi})\rho(-\boldsymbol{\xi})\rangle,$$
$$S^{(3)}(\boldsymbol{\xi},\boldsymbol{\xi}') = \frac{1}{N}\langle \rho(\boldsymbol{\xi})\rho(\boldsymbol{\xi}')\rho(-\boldsymbol{\xi}-\boldsymbol{\xi}')\rangle, \quad \text{etc.} \tag{94}$$

We note that these results are written using the structure factors which are important quantities in condensed matter physics and crystallography since they are directly related to statistical information, i.e the relative arrangement of the inclusions. For example, $S^{(2)}(\boldsymbol{\xi})$ is connected to radial distribution $g^{(2)}(\boldsymbol{r})$ via the expression

$$S^{(2)}(\boldsymbol{\xi}) = 1 + \overline{\rho}\int_V g^{(2)}(\boldsymbol{r})e^{-i\boldsymbol{\xi}.\boldsymbol{r}}d\boldsymbol{r} \tag{95}$$

where $\overline{\rho}$ is the average inclusion density. For a system of non overlapping spheres in equilibrium, analytical expressions for both $g^{(2)}$ and $S^{(2)}$ exist from the solution of Ornstein–Zernike equation (Ornstein and Zernike, 1914) and Percus–Yevick closure approximation (Percus and Yevick, 1958; Wertheim, 1963).*More importantly, $S^{(2)}(\boldsymbol{\xi})$ can be determined experimentally via scattering techniques.* Higher order structure factors like $S^{(3)}$, $S^{(4)}$, ... are more difficult to obtain by experiment (Wochner et al., 2009) but they can be obtained by approximations (Hansen and McDonald, 2006; Nguyen et al., 2016; Barrat et al., 1987; Kirkwood, 1935) or atomistic based computer simulations.

In this work, we are concerned with estimates based on the first two structure factors $S^{(2)}(\boldsymbol{\xi})$ and $S^{(3)}(\boldsymbol{\xi})$ which already perform well. The sums (93) can be rewritten as integrals in the Fourier space as follows

$$\mathbb{D}^1 = \frac{1}{6\pi^2}\int F(\boldsymbol{\xi})F(-\boldsymbol{\xi})\mathbb{B}(\boldsymbol{\xi})S^{(2)}(\boldsymbol{\xi})d\boldsymbol{\eta}$$
$$\mathbb{D}^2 = \frac{1}{36\pi^4}\iint F(\boldsymbol{\xi})F(\boldsymbol{\xi}')F(\boldsymbol{\xi}-\boldsymbol{\xi}')\mathbb{B}(\boldsymbol{\xi})\mathbb{B}(\boldsymbol{\xi}')S^{(3)}(-\boldsymbol{\xi},\boldsymbol{\xi}')d\boldsymbol{\eta}d\boldsymbol{\eta}'. \tag{96}$$

For isotropic distributions of non overlapping spheres, we have the following property

$$\frac{1}{6\pi^2}\int F^2(\xi)S^{(2)}(\xi)d\boldsymbol{\eta} = (1-f) \tag{97}$$

regardless the local pair distribution $S^{(2)}$. As in the discrete case, the expression of the equivalent main shear modulus is given by expression (92), but using the continuous equivalent of S_3 given by:

$$S_3 = \frac{1}{6\pi^2}\int F(\boldsymbol{\xi})F(-\boldsymbol{\xi})\bar{\xi}_i^2\bar{\xi}_j^2S^{(2)}(\boldsymbol{\xi})d\boldsymbol{\eta} \tag{98}$$

Using the general relation (97), we can finally evaluate S_3

$$S_3 = \frac{1-f}{15} \tag{99}$$

and finally (93), giving the first order evaluation of the main shear modulus μ_e coincides with the HS bound for μ_e (Hashin and Shtrikman, 1963). As seen thereafter, the evaluation at the second order departs from HS bound.

4. Numerical applications and analysis

Let us consider the application of our theory to a cubic array of spheres in comparison with FFT and some literature results. From Figs. 4, 5 and Tables 2, 3, we find that the second order estimates have improved significantly the HS bound which coincides with the first order estimates. The degree of improvement depends on the properties considered, estimation scheme, microstructure and the elastic properties of constituents. For BCC array with contrast

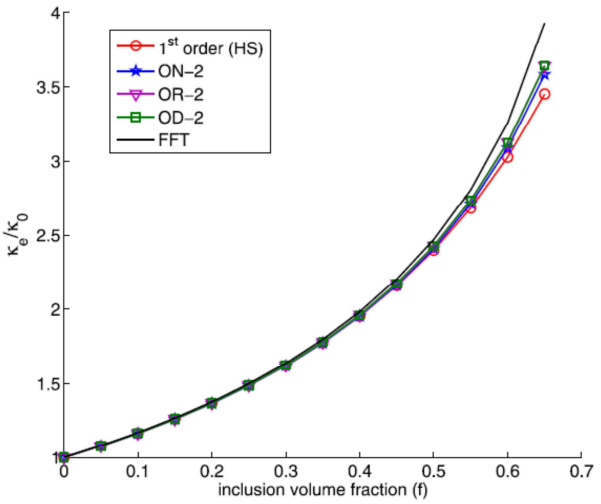

Fig. 4. Normalized effective bulk modulus κ_e/κ_0 vs inclusion volume fraction f of BCC array. Elastic properties of the constituents are $\nu_1 = 0.4$, $\nu_0 = 0.3$, $\mu_1/\mu_0 = 10$. The results are computed by first order estimates which all coincide with HS estimates, second order estimates of the three methods (OR,ON and OD) and the numerical method FFT at convergence.

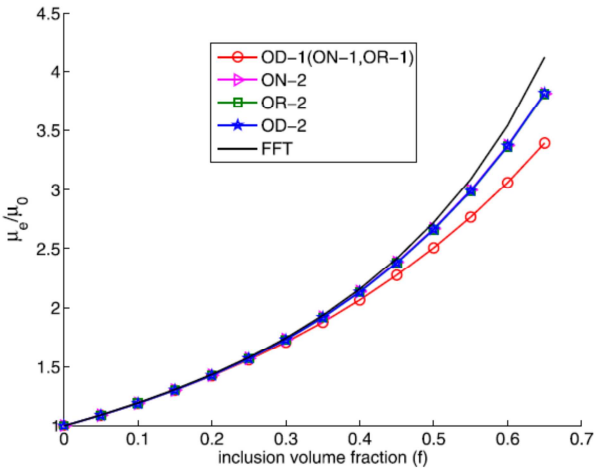

Fig. 5. Normalized effective shear moduli μ_e/μ_0 vs inclusion volume fraction f of BCC array. Elastic properties of the constituents are $\nu_1 = 0.4$, $\nu_0 = 0.3$, $\mu_1/\mu_0 = 10$. The results are computed by first order estimates, second order estimates of the three methods (OR,ON and OD) and the numerical method FFT at convergence.

Table 2
Normalized effective bulk modulus κ_e/κ_0 vs inclusion volume fraction f of FCC. Elastic properties of the constituents are $\nu_1 = 0.4$, $\nu_0 = 0.3$, $\mu_1/\mu_0 = 100$. The results are computed by first order estimates which coincide with HS estimates, second order estimates of the three methods (OR,ON and OD) and the numerical method FFT at convergence.

f	Order 1	ON-2	OR-2	OD-2	FFT
0.10	1.1784	1.1754	1.1791	1.1795	1.1907
0.20	1.4009	1.3950	1.4024	1.4031	1.4254
0.30	1.6863	1.6769	1.6898	1.6911	1.7293
0.40	2.0659	2.0536	2.0758	2.0785	2.1424
0.50	2.5952	2.5872	2.6287	2.6357	2.7533
0.60	3.3850	3.4182	3.5059	3.5276	3.8286
0.70	4.6900	4.9483	5.1744	5.2562	7.2886

Table 3
Effective shear moduli μ_e/μ_0 vs inclusion volume fraction f of FCC. Elastic properties of the constituents are $\nu_1 = 0.4$, $\nu_0 = 0.3$, $\mu_1/\mu_0 = 100$. The results are computed by first order estimates, second order estimates of the three methods (OR,ON and OD) and the numerical method FFT at convergence.

f	Order-1	ON-2	OR-2	OD-2	FFT
0.10	1.2338	1.2348	1.2350	1.2355	1.2523
0.20	1.5365	1.5433	1.5437	1.5457	1.5819
0.30	1.9347	1.9667	1.9675	1.9745	2.0417
0.40	2.4719	2.5742	2.5770	2.5970	2.7232
0.50	3.2230	3.4793	3.4896	3.5381	3.8078
0.60	4.3281	4.8812	4.9222	5.0277	5.5844
0.70	6.0830	7.2978	7.4748	7.7229	10.7332

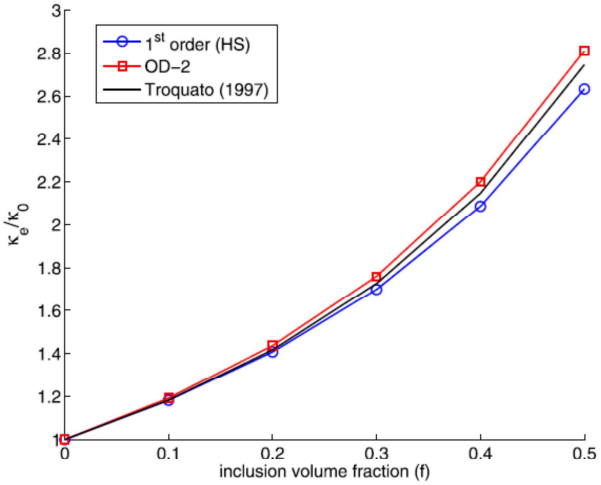

Fig. 6. Normalized effective bulk modulus κ_e/κ_0 vs inclusion volume fraction f for random distribution of rigid spheres ($\mu_1/\mu_0 = \kappa_1/\kappa_0 = \infty$). The solutions of the present work (OD-1, OD-2) are compared with the results of Torquato (1997); 1998). The first order estimates coincide with HS estimates.

ratio as high as 10 (see Fig 4 and 5), the second order estimates of the bulk modulus κ_e/κ_0 and the shear modulus μ_e/μ_0 issued from the three schemes are close to the FFT results at convergence. The agreement is good upto a very high volume fraction near the percolation limit. Detailed results on FCC array also have the same trend as those for BCC cases. Tables 2 and 3 show that the two series OR and OD yield very good results while the series ON works less well. It is interesting to note that at volume fraction as large as 0.5 and the rigidity contrast ratio as high as 100, our three estimates perform well.

Next, we study microstructures constituted of randomly isotropic distribution of spheres. Two extreme cases of rigid spheres and voids will be considered. Fifty sample composed of 500 non overlapping spheres are prepared by standard Event Driven Molecular Dynamics (Rapaport, 2004). To compute the effective properties of the material, we shall limit to OD based estimates and final results are obtained by averaging over the 50 samples. It may be noticed that, the iterative scheme is not theoretically convergent for fields in void or rigid inclusions but the effective properties exist for the considered microstructures. In this case, the expressions for μ_e and κ_e at first and second order can be used for infinite contrast (Fig. 6). Simulations on the systems show that the OD-2 estimate is close to the estimate of Torquato (1998); 1997). For spherical voids (see Fig. 7), our second order estimate again shows a significant improvement with respect to the first order (HS bound). The estimate is also close to

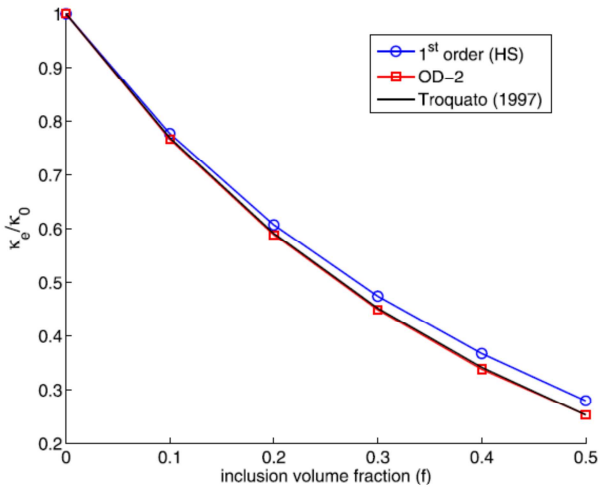

Fig. 7. Normalized effective bulk modulus κ_e/κ_0 vs inclusion volume fraction f with random distributions of spherical voids ($\mu_1/\mu_0 = \kappa_1/\kappa_0 = 0$). The solutions of the present work (OD-1, OD-2) are compared with the results of Torquato (1997); 1998). The first order estimates coincide with HS estimates.

Torquato (1998); 1997) using three point parameters. Those results again confirm the robustness of our estimation scheme at high rigidity contrast and high volume fraction. We note that the good performance comes from the benefit of the fast convergence series and the high order correlation information.

5. Concluding remarks

In this paper, we have presented a new estimate of the overall stiffness tensor of elastic composites. Starting from a class of Lippmann-Schwinger integral equations for eigenstress (or eigenstrain), the optimization procedure is then carried out to find the best Neumann series, i.e those with the fastest convergence rate. To this end, we have introduced tools to bound the spectral radius and norm of fourth order operators in Fourier space and methods to obtain the optimal series. The series are then used to derive estimates at different order n.

We have also shown that $n-$ order statistical information on the microstructure, in this case corresponding to the structure factors, also appear in the estimates. Numerical applications of the procedure on some test cases show that our estimates perform very well in comparison with FFT results and those from the literature.

Not only concerning the theoretical estimates, the contribution of the present paper is closely related to the FFT resolution method. Results issued from the paper correspond to new computation methods based on the eigenstress whose theory is rigorously founded and convergence rate is controllable. Indeed, by not taking the reference material as one of the constituents while keeping all the remaining ingredients, we obtain a very general and promising class of series which can be developed into new FFT schemes. The next step is to optimize and examine the convergence performance in comparison with the existing FFT schemes. Those perspectives will be investigated in a future work.

Acknowledgement

This project is funded by the National Foundation for Science and Technology Development (NAFOSTED) under grant number 107.02-2016.05.

Appendix A. Lippmann–Schwinger equations in elasticity and associated FFT resolution method

The boundary value problem can be solved using either one of the two Lippmann–Schwinger integral equations

$$\boldsymbol{\epsilon} = \boldsymbol{E} - \boldsymbol{\Gamma}^0 \delta' \mathbb{C}\boldsymbol{\epsilon}, \quad \boldsymbol{\sigma} = \boldsymbol{\Sigma} - \boldsymbol{\Delta}^0 \delta' \mathbb{S}\boldsymbol{\sigma} \tag{A.1}$$

It is clear that these two integral equations are equivalent to (29) and (30) via the relations $\boldsymbol{\tau} = \delta' \mathbb{C}\boldsymbol{\epsilon}$ and $\boldsymbol{e} = \delta' \mathbb{S}\boldsymbol{\sigma}$. Taking the first equation (A.1) as an example, $\boldsymbol{\epsilon}$ can be computed by repeating the iterative scheme

$$\boldsymbol{\epsilon}^0 = \boldsymbol{E}, \quad \boldsymbol{\epsilon}^{n+1} = \boldsymbol{E} - \boldsymbol{\Gamma}^0 \delta' \mathbb{C}\boldsymbol{\epsilon}^n \tag{A.2}$$

until convergence. Since we know the explicit expression of $\boldsymbol{\Gamma}^0$ in the Fourier space and the material distribution $\delta' \mathbb{C}$ in the physical space, it is preferable to use the FFT algorithm to convert results back and forth between the two spaces. In most of our applications, the resolution $256 \times 256 \times 256$ is adopted for both spaces. Finally, improving the resolution and increasing the number of iterations up to convergence, we obtain the exact solution of the problem within any given accuracy. We note that the adopted FFT method is related to ES series and different from series used as the background of the estimation presented in the paper. Using this classic scheme, the bulk stiffness and the shear stiffness of the reference material are chosen as averages (half sums) of the related moduli of inclusion and matrix. Details of the scheme can be found in previous works (Michel et al., 1999; Bonnet, 2007).

Appendix B. Method of computing $\mathbb{D}^n$ and explicit expressions for $\mathbb{D}^1$

To compute numerically tensor $\mathbb{D}^n$ ($j \geq 1$), we need to base on (75) which can be recast as

$$\begin{aligned} &\mathbb{D}^j = f^{-1} \sum_{\xi} \chi(\boldsymbol{\xi}) \mathbb{F}^j(\boldsymbol{\xi}) \chi(-\boldsymbol{\xi}), \\ &\mathbb{F}^1(\boldsymbol{\xi}) = \mathbb{B}(\boldsymbol{\xi}), \quad \mathbb{F}^j(\boldsymbol{\xi}) = \mathbb{B}(\boldsymbol{\xi})(\chi * \mathbb{F}^{j-1})(\boldsymbol{\xi}), \quad j \geq 2, \end{aligned} \tag{B.1}$$

where * stands for convolution in Fourier space. Given the explicit expressions of $\mathbb{B}$ and χ in Fourier space, the convolution can be done efficiently using FFT techniques.

To compute the cubic tensor $\mathbb{D}^1$, we need to calculate first the following elementary $\mathbb{H}^i$ using Walpole base elements $\mathbb{E}^i$

$$\mathbb{H}^i = f^{-1} \sum_{\xi} \mathbb{E}^i(\boldsymbol{\xi}) \chi(\boldsymbol{\xi}) \chi(-\boldsymbol{\xi}), \quad i = 1, 2, .., 6 \tag{B.2}$$

The explicit Mandel matrix representation of those tensors in terms of S_1, S_2 and S_3 are given as follows

$$[\mathbb{H}^1] = \begin{bmatrix} \frac{1}{2}(S_1+S_2) & \frac{1}{2}(S_1+S_3) & \frac{1}{2}(S_1+S_3) & 0 & 0 & 0 \\ \frac{1}{2}(S_1+S_3) & \frac{1}{2}(S_1+S_2) & \frac{1}{2}(S_1+S_3) & 0 & 0 & 0 \\ \frac{1}{2}(S_1+S_3) & \frac{1}{2}(S_1+S_3) & \frac{1}{2}(S_1+S_2) & 0 & 0 & 0 \\ 0 & 0 & 0 & S_3 & 0 & 0 \\ 0 & 0 & 0 & 0 & S_3 & 0 \\ 0 & 0 & 0 & 0 & 0 & S_3 \end{bmatrix}, \tag{B.3}$$

$$[\mathbb{H}^2] = \begin{bmatrix} S_2 & S_3 & S_3 & 0 & 0 & 0 \\ S_3 & S_2 & S_3 & 0 & 0 & 0 \\ S_3 & S_3 & S_2 & 0 & 0 & 0 \\ 0 & 0 & 0 & 2S_3 & 0 & 0 \\ 0 & 0 & 0 & 0 & 2S_3 & 0 \\ 0 & 0 & 0 & 0 & 0 & 2S_3 \end{bmatrix}, \tag{B.4}$$

$$[\mathbb{H}]^3 = \begin{bmatrix} \frac{1}{2}(S_1+S_2) & \frac{1}{2}(S_3-S_1) & \frac{1}{2}(S_3-S_1) & 0 & 0 & 0 \\ \frac{1}{2}(S_3-S_1) & \frac{1}{2}(S_1+S_2) & \frac{1}{2}(S_3-S_1) & 0 & 0 & 0 \\ \frac{1}{2}(S_3-S_1) & \frac{1}{2}(S_3-S_1) & \frac{1}{2}(S_1+S_2) & 0 & 0 & 0 \\ 0 & 0 & 0 & S_1+S_3 & 0 & 0 \\ 0 & 0 & 0 & 0 & S_1+S_3 & 0 \\ 0 & 0 & 0 & 0 & 0 & S_1+S_3 \end{bmatrix}, \tag{B.5}$$

$$[\mathbb{H}]^4 = \begin{bmatrix} 2(S_1-S_2) & -2S_3 & -2S_3 & 0 & 0 & 0 \\ -2S_3 & 2(S_1-S_2) & -2S_3 & 0 & 0 & 0 \\ -2S_3 & -2S_3 & 2(S_1-S_2) & 0 & 0 & 0 \\ 0 & 0 & 0 & 2(S_1-2S_3) & 0 & 0 \\ 0 & 0 & 0 & 0 & 2(S_1-2S_3) & 0 \\ 0 & 0 & 0 & 0 & 0 & 2(S_1-2S_3) \end{bmatrix}, \tag{B.6}$$

$$[\mathbb{H}]^5 = [\mathbb{H}]^6 = \begin{bmatrix} S_1-S_2 & S_1-S_3 & S_1-S_3 & 0 & 0 & 0 \\ S_1-S_3 & S_1-S_2 & S_1-S_3 & 0 & 0 & 0 \\ S_1-S_3 & S_1-S_3 & S_1-S_2 & 0 & 0 & 0 \\ 0 & 0 & 0 & -2S_3 & 0 & 0 \\ 0 & 0 & 0 & 0 & -2S_3 & 0 \\ 0 & 0 & 0 & 0 & 0 & -2S_3 \end{bmatrix}, \tag{B.7}$$

From the above results, given any tensor $\mathbb{B}(\boldsymbol{\xi})$ with representation $\mathbb{B}(\boldsymbol{\xi}) = \sum_{i=1}^{6} b_i \mathbb{E}^i(\boldsymbol{\xi})$, we can derive $\mathbb{D}^1 = \sum_{i=1}^{6} b_i \mathbb{H}^i$ and the parameters α_1 and β_1 in (88).

References

Barrat, J.L., Hansen, J.P., Pastore, G., 1987. Factorization of the triplet direct correlation function in dense fluids. Phys. Rev. Lett. 58, 2075.

Bhattacharya, K., Suquet, P., 2005. A model problem concerning recoverable strains of shape-memory polycrystals. Proc. R. Soc. A 461, 2797–2816.

Bonnet, G., 2007. Effective properties of elastic periodic composite media with fibers. J. Mech. Phys. Solids 55, 881–899.

Brisard, S., Dormieux, L., 2010. Fft-based methods for the mechanics of composites: a general variational framework. Compu. Mat. Sci. 49, 663–671.

Christensen, R., Lo, K., 1979. Solutions for effective shear properties in three phase sphere and cylinder models. J. Mech. Phys. Solids 27, 315–330.

Eshelby, J., 1957. The determination of the elastic field of an ellipsoidal inclusion, and related problems. Proc. R. Soc. A 241, 376–396.

Eyre, D.J., Milton, G.W., 1999. A fast numerical scheme for computing the response of composites using grid refinement. Eur. Phys. J. Appl. Phys. 6, 41–47.

Hansen, J.P., McDonald, I.R., 2006. Theory of Simple Liquids. Academic press.

Hashin, Z., Shtrikman, S., 1963. A variational approach to the theory of the elastic behaviour of multiphase materials. J. Mech. Phys. Solids 11, 127–140.

Kirkwood, J.G., 1935. Statistical mechanics of fluid mixtures. J. Chem. Phys. 3, 300–313.

Michel, J., Moulinec, H., Suquet, P., 1999. Effective properties of composite materials with periodic microstructure: a computational approach. Comput. Method Appl. Mech. Eng. 172, 109–143.

Michel, J., Moulinec, H., Suquet, P., 2001. A computational scheme for linear and non-linear composites with arbitrary phase contrast. Int. J. Numer. Meth. Eng. 52, 139–160.

Milton, G.W., 2002. The Theory of Composites. Volume 6. Cambridge University Press.

Monchiet, V., Bonnet, G., 2012. A polarization-based FFT iterative scheme for computing the effective properties of elastic composites with arbitrary contrast. Int. J. Numer. Meth. Eng. 89, 1419–1436.

Mori, T., Tanaka, K., 1973. Average stress in matrix and average elastic energy of materials with misfitting inclusions. Acta. Metall. Mater. 21, 571–574.

Nemat-Nasser, S., Iwakuma, T., Hejazi, M., 1982. On composites with periodic structure. Mech. Mater. 1, 239–267.

Nguyen, M.T., Monchiet, V., Bonnet, G., To, Q.D., 2016. Conductivity estimates of spherical-particle suspensions based on triplet structure factors. Phys. Rev. E 93, 022105.

Ornstein, L., Zernike, F., 1914. Accidental deviations of density and opalescence at the critical point of a single substance. Proc. Acad. Sci. Amsterdam 17, 793–806.

Percus, J.K., Yevick, G.J., 1958. Analysis of classical statistical mechanics by means of collective coordinates. Phys. Rev. 110, 1.

Rapaport, D., 2004. The Art of Molecular Dynamics Simulation. Cambridge University Press.

Sanchez-Palencia, E., 1980. Non-Homogeneous Media and Vibration Theory. Lecture Notes in Physics, vol. 127. Springer Verlag, Berlin.
To, Q.D., Bonnet, G., 2014. A numerical-analytical coupling computational method for homogenization of effective thermal conductivity of periodic composites. Asia Pac. J. Comput. Eng. 1, 5.
To, Q.D., Bonnet, G., Hoang, D.H., 2016. Explicit effective elasticity tensors of two-phase periodic composites with spherical or ellipsoidal inclusions. Int. J. Solids Struct. 94–95, 100–111.
Torquato, S., 1997. Effective stiffness tensor of composite media. I. Exact series expansions. J. Mech. Phys. Solids 45, 1421–1448.
Torquato, S., 1998. Effective stiffness tensor of composite media : II. Applications to isotropic dispersions. J. Mech. Phys. Solids 46, 1411–1440.
Torquato, S., 2001. Random Heterogeneous Materials: Microstructure and Macroscopic Properties. Springer, Berlin.
Walpole, L., 1981. Elastic behavior of composite materials: theoretical foundations. Adv. Appl. Mech. 21, 169–242.
Wertheim, M., 1963. Exact solution of the Percus-Yevick integral equation for hard spheres. Phys. Rev. Lett. 10, 321–323.
Wochner, P., Gutt, C., Autenrieth, T., Demmer, T., Bugaev, V., Ortiz, A.D., Duri, A., Zontone, F., Grübel, G., Dosch, H., 2009. X-ray cross correlation analysis uncovers hidden local symmetries in disordered matter. Proc. Natl. Acad. Sci. 106, 11511–11514.